ACS Catalysis

Review

pubs.acs.org/acscatalysis

Modern Trends in Catalyst and Process Design for Alkyne Hydrogenations

Micaela Crespo-Quesada, Fernando Cárdenas-Lizana, Anne-Laure Dessimoz, and Lioubov Kiwi-Minsker*

Group of Catalytic Reaction Engineering, École Polytechnique Fédérale de Lausanne (EPFL), CH-1015 Lausanne, Switzerland

ABSTRACT: This review provides an overview of the recent achievements in catalytic process development for alkyne hydrogenations. It underlines the necessity of simultaneous optimization over different length scales from molecular/nanoscale of active phase, up-to macro-scale of catalytic reactor design. One case study, the hydrogenation of 2-methyl-3-butyn-2-ol, is analyzed in detail to illustrate the practical application of this approach. Finally, it presents the personal view of the authors concerning the new trends and paths available in the field.

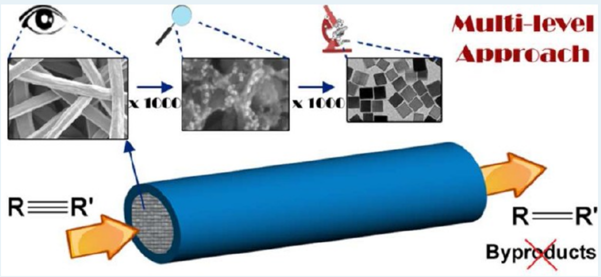

KEYWORDS: *alkyne, hydrogenation, catalyst design, support effect, reactor design*

1. INTRODUCTION

Sustainable processing with minimal environmental impact has been recognized as one of the major challenges of this century.[1] As a result of the severe restrictions in environmental legislation, the chemical industry is now undergoing a progressive redefinition. Catalytic technology, as a fundamental tool for green chemistry, has an unprecedented enabling potential for sustainable production. Heterogeneous catalysts are of utmost importance in the fine chemical industry. The typical design in these systems is based on an active phase, main responsible for the catalytic performance (activity and selectivity), immobilized on a suitable support. This avoids agglomeration of the active species during chemical reaction and enables an easy catalyst recovery. The conventional methodology applied for catalyst optimization has been an empirical "trial-and-error" approach which results, at best, in slight or incremental improvements of their performance. Moreover, it is greatly based on speculation and is, in practice, laborious and time-consuming. With the concomitant advance in theoretical understanding and the development of computational power, a new era of *rational catalyst design* (RCD) is dawning.[2] This approach is based on a multidisciplinary combination of new advances in synthesis, characterization, and modeling with the ultimate aim of predicting the catalyst's behavior based on chemical composition, molecular structure, and morphology.[3]

Given the multicomponent nature of an heterogeneous catalyst, it is necessary to bear in mind that its overall performance depends not only on the contribution of the active component, but also on other factors such as the interplay between the catalytically active species and the surrounding environment, and the type of chemical reactor where the process is carried out (Figure 1). Therefore, RCD must span over multiple levels of complexity, from the molecular or nanoscale involving the design of the active sites to the macro-scale design of the industrial reactor where the catalyst is bound to operate, since they are in direct interaction influencing the overall performance.

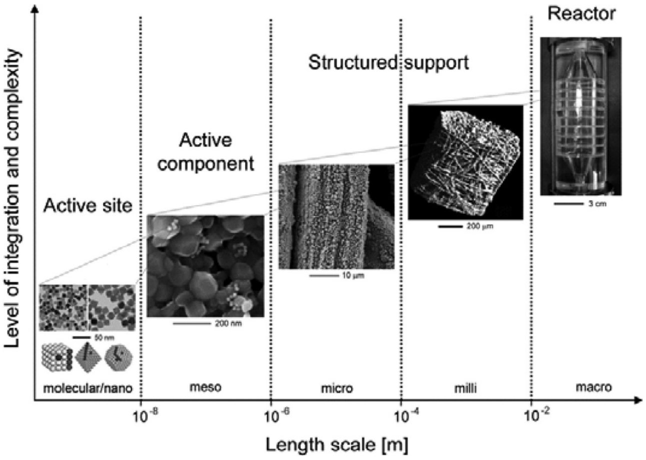

Figure 1. Rational catalyst design spans over several levels of scale and complexity.[2]

The catalytic partial hydrogenation (semi-hydrogenation) of alkynes is of special relevance in the bulk and fine chemical industries[4] since it is an efficient method for production of alkenes. This process is conventionally performed over quinoline-promoted $CaCO_3$ supported Pd catalyst partially poisoned with lead, which is known as Lindlar's catalyst.[5,6] However, the application of this conventional catalytic system to alkyne hydrogenations is sometimes problematic because of selectivity issues (overhydrogenation to alkanes), limited catalyst robustness, and reuse. Moreover, catalyst deactivation, the presence of toxic lead, and the need for the addition of an

Received: May 4, 2012
Revised: June 29, 2012
Published: July 11, 2012

Table 1. Compilation of Literature on Gas-Phase Alkyne Hydrogenation

reaction			nanolevel		meso-level/macro-level		
reactant(s)	P (bar) ; T (K)	X (%); $S_{C=C}$ (%)	metal	stabilizer (modifier)	powder vs [structured] support(s)	reactor	ref.
acetylene	1 ; 298–673	0–100; 45–100	Au		Al_2O_3; α-Fe_2O_3; CeO_2	gas circulation system/single pass flow reactor/fixed-bed microreactor	8–10
	1–16 ; 303–453	<5–100; 0–100	Au; Ag ; Pd; Pd–Au; Pd–Ag; Pd–Cu		TiO_2; Al_2O_3	flow reactor/microreactor	11–13
	1 ; 343–423	10–25 ; 35–85	Pd	IL[a], PVP[b], KBr	[CNF; ACF][c]	pulse-flow reactor/jacketed tubular fixed-bed reactor	14–16
	1 ; 523	100; 25–80	Cu–Fe;Cu–Ni–Fe		HT[d]	fixed-bed microreactor	17
acetylene+ethylene	1 ; 298	50; 49–76	Pd		active carbon	nongradient flow	18
	1 ; 283–353	0–100; >95	Pd ; Ni–Zn		pumice; SiO_2; Al_2O_3; $MgAl_2O_4$	gradientless microreactor/tubular fixed-bed reactor	19–23
acetylene and acetylene+ethylene	1 ; 298–613	<5–99; 60–85	Pd–Ga[e] ; Pd ; Pd–Ag[e]		IC[e]; Al_2O_3	pulse-flow reactor	24,25
phenylacetylene +Styrene	1 ; 423	5–100; 2–98	Au		γ-Al_2O_3	flow reactor	26
propyne	1 ; 273–298	10–100 ; 48–100	Pd ; Pt		ZrO_2; SiO_2; Al_2O_3	pulse-flow reactor	27,28
	1 ; 363–623	0–63; 18–100	Cu ; Au[f]		SiO_2; MgO; (α-,γ)Al_2O_3; ZrO_2; TiO_2; Fe_2O_3; SiO_2–Al_2O_3	dynamic flow/pulse-flow reactor	29,30
	1 ; 373–523	0–100; 0–92	Ni–Al ; Cu	(CO)	HT[d]	fixed-bed microreactor	31,32
	1 ; 423–523	5–100; 30–100	Cu ; Cu–Fe; Cu–Al ; Cu–Ni–Fe; Cu–Ni–Al		HT[d]; SiO_2; Al_2O_3	fixed-bed microreactor	17,33
propyne+propadiene	1 ; 363–553	3–100; 20→99.5	Cu		SiO_2	dynamic flow	34
but-1-yne	0.06–0.20; 293–333	65–69; 40–74	Ni		pumice	static constant volume system	35
	0.07–0.11; 313–493	58–88, 10–100	Ni; Cu; Ni–Cu[f]			static constant volume system	36
	1; 255–293	3–100; <5–90	Pt ; Pt–Ru		Al_2O_3; SiO_2	glass flow	37–39
but-1-yne; 1-butene-3-yne	1 ; 373–513	35–100; 25–60 100; 24	Cu		SiO_2	fixed-bed flow microreactor	40,41
2-methyl-1-buten-3-yne	1 ; 278–323	15–80 ; 25–98	Pd-X[g]		α-Al_2O_3	flow reactor	42
	1 ; 348	10–100; 0–100	Pd; Pd–Pb; Cu; Ni ; Cu–Ni	(CO)	γ-Al_2O_3; $CaCO_3$; HT[d]	fixed-bed microreactor	43
	1; 348	100; 85	Pd–Pb		$CaCO_3$ (Lindlar)	fixed-bed microreactor	43
1-Pentyne	0.9 × 10^{-3}–1 ; 308–373	2–100; 0–100	Pd black; Pd		θ-Al_2O_3; ZnO; SiO_2; Al_2O_3; CNT[h]	continuous-flow microreactor	44–47

[a] IL = ionic liquid. [b] PVP = poly(vinylpyrrolidone). [c] CNF = carbon nanofibers, ACF = activated carbon fibers. [d] HT = hydrotalcite. [e] IC = intermetallic unsupported compound. [f] catalysts provided by the World Gold Council. [g] X = Ge, Sb, Sn, Pb. [h] CNT = cabon nanotubes.

Table 2. Compilation of Literature on Liquid-Phase Alkyne Hydrogenation

reaction			nanolevel		meso-level/macro-level		
reactant	P (bar);T (K)	X (%) ; $S_{C=C}$ (%) [Y(%)]	metal	stabilizer (modifier)	powder vs [structured] support(s)	reactor	ref.
1-hexyne	1–10.5 ; 298–303	85–100 ; 98.5	Pd	AOT^{a}, bipy^{b}, PVP^{c} (Bi, Pb)	[CNF/SMF]^{d}, Al_2O_3,	semibatch	48–51
	10.5 ; 303	99 ; 87	Pd		$CaCO_3$ (Lindlar)	semibatch	49
1-hexyne 1-pentyne	1 ; 298	33–78 ; 96–99	Pt	CTAB^{e}	MCM-41^{f}	vibration reactor	52
2-hexyne	5 ; 353	10–100 ; 20–95	PdO_xH_y	PVP^{c}	C, SiO_2, Al_2O_3, TiO_2	multibatch	53
	1 ; 333–393	7–90 ; 63–99	Pt	PVP^{c}	TiO_2, AMMSiTi^{g}	membrane semibatch	54,55
	1 ; 298	^{h}	Pd	phenanthroline, PVP^{c} (Bi, Pb)	TiO_2, Al_2O_3, $CaCO_3$	semibatch	50,51,56
	1 ; 298	[100]	Pd		$CaCO_3$ (Lindlar)	semibatch	50
3-hexyne 3-hexyn-1-ol	1–2.8 ; 283–298	40–100 ; 85–100	Pd	PVP^{c}, Surfactants, IL^{i} (Rh, Ru, Ag, Cu, Pb)	C, $CaCO_3$, Al_2O_3, CeO_2, SBA-15^{j}, MCM-48^{j}, MSU γ-Al_2O_3^{k}, graphite oxide	semibatch Fisher–Porter bottle vibration reactor	51,57–60
MBY	2–10 ; 308–348	10–99 ; 77–99 [>95]	Pd	PVP^{c}, Na_2MoO_4, AOT^{a}, CTAB^{e} (S-CC^{l}, quinoline)	[ZnO/SMF]^{d}, ZnO	semibatch	61–66
	1 ; 328–337 5 ; 333	96–100 ; 81–97	Pd PdZn	(pyridine)	TiO_2	microreactor semibatch	67
	2–6.7 ; 308–343	22–48^{h}	Pd		[ZnO/SMF]^{d}	SBCR^{m}	68
	5 ; 343	95 ; 97.5	Pd		$CaCO_3$ (Lindlar)	semibatch	62
2-butyne-1,4-diol	1–6 ; 303–323	80 ; 15–59 [94]	Pd	PEO-b-P2VP^{n}	γ-Al_2O_3, C	semibatch	69,70
	2.4 ; 323	100 ; 91–99 100 ; 65–85	Pt, Rh, Ru, Pd and Ni	PVP^{c}	- $CaCO_3$, C	semibatch	71
MPY	1–2.3 ; 298	6 ; 95 [54–97]	Pd	(Cu, quinoline, KOH)	silica, [monoliths], CNF^{d}, SiO_2	semibatch microreactor	72–75
4-octyne	1–8 ; 283–303	4–100 ; 95–100 [91–99]	Pd	CTAB^{e}, SDS^{o} ((n-$C_4H_9)_4NBH_4$)	graphite oxide, C, HT^{p}, Al_2O_3, Montmorillonite	semibatch vibration reactor	59,76–78
phenylacetylene	1–20 ; 283–333	4–100 ; 10–100 [>95]	Pd		C, CNT^{q}, AC^{r} [Si foam] γ-Al_2O_3, MCM-41^{f} Montmorillonite	semibatch	78–83
	1 ; 283	15 ; 80	Pt	(Sn)	Nylon, C	semibatch	84
	7 ; 333	8–100 ; 83–91	Rh	PVP^{c} (PPh_3)		Fisher–Porter bottle	85

[a] AOT = sodium di-2-ethylhexylsulfosuccinate. [b] bipy = bipyridine. [c] PVP = poly(vinylpyrrolidone). [d] CNF = carbon nanofibers, SMF = sintered metal fibers. [e] CTAB = cetyltrimethylammonium bromide. [f] Mesoporous silica. [g] AMMSiTi = amorphous microporous titania-silica mixed oxide. [h] Information not provided. [i] Ionic liquids. [j] Mesoporous silica. [k] Mesoporous gamma alumina. [l] S-CC = Sulfur containing compound. [m] SBCR = staged bubble column reactor. [n] PEO-b-P2VP = poly(ethylene oxide)-block-poly-2-vinylpyridine. [o] SDS=Sodium dodecyl sulfate. [p] HT= hydrotalcite. [q] CNT=carbon nanotubes. [r] AC=activated carbon.

amine modifier are the main drawbacks of this catalytic system.[7] Therefore, during the past few years a significant number of publications were devoted to alkyne hydrogenation processes. Given the requirement of the simultaneous consideration of different levels for optimum catalytic process design, this review is focused on the analysis of the different scale lengths (*nano*, *micro*, and *macro*) applied to the catalytic selective C≡C to C═C hydrogenation with special emphasis on the literature published over the past decade.

Instead of merely providing an enumeration of the articles dealing with catalytic *semi*-hydrogenation over the different *scale* lengths, a representative compilation of studies is given in Tables 1 and 2 for gas and liquid phase operations, respectively.

The information shown serves to illustrate (a) the range of reactions that have been investigated; (b) the operating temperatures and pressures; (c) the catalytic performance in terms of activity (presented as conversion (X)) and product distribution (in terms of selectivity (S_i) or yield (Y)); (d) the nature of the catalytic systems that have been investigated at different scale lengths, that is, nano (metal and precursor/stabilizer), meso (support), and macro-level (reactor).

Of direct relevance to this work, we should mention the overview on hydrogenation of carbon−carbon multiple bonds published by Molnár and co-workers in 2001,[86] which has since been supplemented by the reports of Borodziński and Bond[87,88] on selective hydrogenation of ethyne in ethene-rich streams over palladium catalysts, and the recent examination of the theoretical work to elucidate the catalytic properties required for selective alkyne hydrogenation in mixtures by López and Vargas Fuentes.[89] The critical role of a combined (catalyst, process and reactor) design strategy for optimizing heterogeneous catalysis was illustrated in a review by Sie and Krishna in 1998,[90] which has been since covered in more recent publications.[2,91]

This Review contains two main parts. First, a critical analysis of the pertinent literature dealing with catalyst design for selective C≡C to C═C hydrogenations across the three scale lengths previously reported is provided and new trends are underlined. In the second part, a case study, the hydrogenation of 2-methyl-3-butyn-2-ol (MBY) is presented for illustrative purposes. Finally, the Review ends with a consideration of directions for the future.

2. MULTI-LEVEL APPROACH FOR CATALYTIC ALKYNE HYDROGENATION

The selective C≡C hydrogenation (to the correspondent olefin) is an important process in industry for both the production of intermediates in the manufacture of fine chemicals,[63] and in bulk chemistry, for example, ethylene hydrogenation during the synthesis of polyethylene (global annual production of 50 million tons[92]) and the purification of alkene streams for the upgrade of low weight fractions from stream crackers.

The open literature on selective alkyne hydrogenation reports the process carried out in both gas (see Table 1) and liquid-phase (see Table 2). It can be seen that this type of reaction has been primarily carried out over powdered catalysts based on monometallic Pd and, to a lesser extent, Pt-, Ni-, Cu-, and Au-based catalysts where the last two metals show promise in terms of achieving high selectivity.[9,17,32] Focusing on Pd as the metal with the best performance for this type of reaction,[5−7] the increased alkene selectivity over Pd can be associated with the distinct alkyne/alkene adsorption energies.[93] Indeed, despite the faster olefin hydrogenation over Pd with respect to the acetylenic counterpart, the reduction of the latter is favored as a result of the increased adsorption strength, that is, the selectivity has a thermodynamic nature.[94]

Several factors have been proposed to control a catalyst's performance in alkyne hydrogenations involving the different scale lengths of the catalyst architecture:

- Nanoscale, where the effect of the morphology of the active nanoparticles is considered through the observation of metal dispersion,[14,20,47,48,63,64,79,87] shape effects,[64,71] and/or the presence of specific types of active sites.[61] Surface modification by the reaction medium is also important at this stage of optimization.[16,44,95]
- Mesoscale, where the interactions between the active metal nanoparticle and its intimate environment is assessed through the modification by alloying,[46,63] the involvement of additives,[32,49,69,96] and/or metal/support interactions.[28,30]
- Micro/milli/macro-scale design where the support structure and morphology are tailored according to the particular requirements of the reaction in conjugation with the development of a suitable chemical reactor.[68]

2.1. Active Phase Optimization: Nano/Meso-Level.

One of the key factors affecting the catalytic behavior of the active phase is the interplay between its properties and the reacting molecules. Therefore, to achieve a fundamental understanding of catalytic reactions, surface-science experiments[44−47] and theoretical calculations[23,33,93,95,97] are required to provide insights into surface dynamics and the nature of the adsorbed species. A quintessential work steering in this direction in which density functional theory (DFT) calculations are used to identify potential new catalysts for the selective hydrogenation of acetylene was recently published.[23] The authors proposed Ni−Zn as an optimal alternative formulation with respect to the conventional Pd-based active phase, which was subsequently corroborated experimentally. Despite the undeniable usefulness of such work, the results should be somehow considered carefully since the formation of oligomers during acetylene hydrogenation was neglected in their calculations.

Although surface and theoretical analyses can provide an additional tool for catalyst optimization, there is still a gap in terms of expected and obtained response when moving to real catalytic systems. Nanoparticle morphology has been identified as a key characteristic linked to the active phase for the hydrogenation of alkynes where differences in catalytic performance have associated to mechanistic, electronic, and/or geometric effects.[98−100] The incorporation of a second metal or specific compound has also proved an effective means to influence selectivity and activity in C≡C hydrogenation.

This section reviews the results of nanoscaled studies for catalytic alkyne hydrogenations considering first the active phase alone, particularly the issue of structure sensitivity, and of active phase modification under reaction conditions. Second, the modification of the active nanoparticles through alloying and additives is also reviewed.

2.1.1. Structure Sensitivity. The morphology (shape and size) of the active phase (metal nanoparticles) is among the structural features that have a greater impact on catalytic performance in alkyne hydrogenation.[101] In the 1960s it had become clear that the rate of certain catalytic reactions, expressed per unit area, or turnover frequency (TOF), was independent of the metal particle size and were defined as *structure-insensitive*. On the other hand, if a correlation between

TOF and metal dispersion could be established, the reaction was then referred to as *structure-sensitive*. It is however more likely that every reaction will show a degree of structure sensitivity, depending on the stringency of its requirements for an active center.[102] It is worth mentioning that a variation in shape also implies important morphological differences: cubes only present (100) plane atoms, octahedra solely (111) plane atoms whereas a mixture of both can be found in cube-octahedra (sphere). This will provoke another type of structure-induced effect, that is, a shape effect, particularly if each type of surface atom possesses a different reactivity.

The first study tackling the issue of nanoparticle *size effects* was published in 1983 by Boitiaux et al.[103] Since then, we have come to realize that a key requirement for structure sensitivity studies calls for the preparation of catalysts which differ only in particle size and/or shape. Typical catalysts are based on supported metal nanoparticles where size control of the metal phase has been achieved by modifications in the nature of the precursors, supports or preparation conditions. As a result, not only size but other important chemical and structural properties of the catalyst that affect catalytic performance are also modified. Therefore, the early data published on size effects in the selective hydrogenation of multiple carbon−carbon bonds are rather controversial, although some consensus emerges pointing toward higher activity for larger particles, that is, an increase in metal dispersion decreases TOF.[14,18,20,47,48,64,65,79] Small nanoparticles (less than 2 nm) are characterized by a predominance of surface atoms of low coordination number characterized by an electron density deficiency. The low activity can be explained on the basis of strong complexation of the surface atoms by the highly unsaturated electron-rich alkyne. Furthermore, it is known that Pd can absorb hydrogen at room temperature when the partial pressure exceeds 0.02 atm resulting in the formation of β-palladium hydride.[104] Hydride formation is the result of hydrogen diffusion in the Pd crystallite structure to occupy the available octahedral "vacancies" in the metal lattice. The relationship between the number of Pd atoms in the bulk crystal with respect to those on the surface, decreases with decreasing particle size to attain a limiting value (<2.5 nm), where H_{ab}/Pd is close to zero.[105,106] The influence of this phase in alkyne hydrogenation is still rather controversial with reports in the literature suggesting that it is responsible for the direct alkane formation[99] while others did not observe this detrimental effect,[100] although a recent publication reports theoretical calculations showing the great importance of subsurface species in alkyne hydrogenations.[95]

In terms of Pd nanoparticle *shape effects,* there is limited work available in the open literature, particularly for alkyne hydrogenation.[107,108] Unlike size, shape control was only recently achieved in a straightforward manner thanks to colloidal techniques.[107−109] The advances in colloidal preparation of metal nanostructures open new opportunities in the study of structure-sensitive reactions since they provide catalytic metal particles with size or shape variation without other perturbations, thus rendering them excellent materials suitable for catalytic investigations. For example, Telkar et al.[71] concluded a dependency between shape and activity (in terms of TOF) for cubic and spherical nanoparticles in the hydrogenation of 2-butyne-1,4-diol. In contrast, in the hydrogenation of 2-methyl-3-butyn-2-ol catalytic performance was found to be insensitive to the nanoparticle shape (nanohexagons vs nanospheres) but dependent on the number of Pd atoms located on (111) planes.[64]

We can therefore conclude that an accurate identification of the active sites responsible for the catalytic performance would actually imply a *redefinition* of the terms "size" and "shape effects" to "structure effect" arising from the relative amount of active sites on the nanoparticle surface regardless of the shape or size of the crystallite. This is illustrated in recent studies for the hydrogenation of 2-methyl-3-butyn-2-ol where it has been shown that the dependency between TOF and particle size disappeared when only Pd_{111}, that is, the active sites for the reaction, is taken into account.[64,65] This finding is complemented by our recent work[61] where, for the same reaction, we have shown for a series of Pd nanoparticles with well-defined shapes and sizes (see Figure 2) that two type of active sites, that is, plane and edge atoms, are responsible for the catalytic performance. Indeed, the existence of two or more different kinds of active sites responsible for observed size and/or shape effects has not been thoroughly discussed in the literature.[102] This fundamental knowledge has a significant potential for catalyst optimization for industrially important hydrogenations. The study of the reaction on well-defined catalysts allows the full kinetic description of the system, and it therefore enables the prediction of the size and shape of the active phase to maximize catalytic efficiency.[61] Only with the new developments in the *nanoscaled architecture* of the catalyst with the blooming of simple and versatile colloidal methods of nanoparticle preparation were these achievements possible.

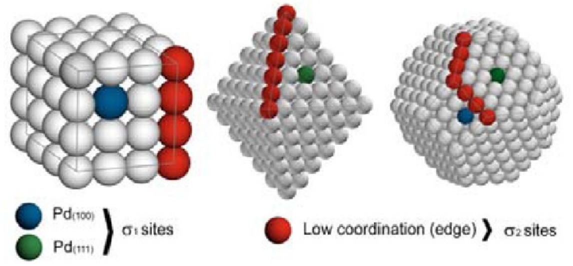

Figure 2. Types of active sites in the hydrogenation of 2-methyl-3-butyn-2-ol (MBY). Plane atoms, regardless of their crystallographic orientation, σ_1 and low coordination or edge atoms, σ_2. Reprinted with permission from ref 61. Copyright (2011) American Chemical Society.

Additional complications can arise for reactions in gas (relative to liquid) phase operation as a result of the more demanding conditions, for example, increased reaction temperatures, which can influence the surface chemistry of the nanoparticles. Much effort has been devoted in this direction to the investigation of the structure sensitivity of acetylene hydrogenation as illustrated in Table 1.[14,15,110] However, it is now almost unanimously accepted that the observed differences are linked to the formation of a carbonaceous overlayer on the surface of Pd.[28,39,44,47] This has been confirmed by both experimental (XPS[44]) and theoretical (DFT calculations[111]) analyses. It was first suggested that the deposited carbon was only a selectivity modifier through site isolation envisaging sites of different sizes between carbon deposits.[20−22,39,112] However, this has been recently revoked in studies showing the formation of carbide species in the subsurface region of the crystallite that prevent the dissolution of hydrogen in the bulk of the nanoparticle,[44,45,47,95] that is, eliminates the source of unselective hydrogenation (Figure 3).[44,47] It must be however

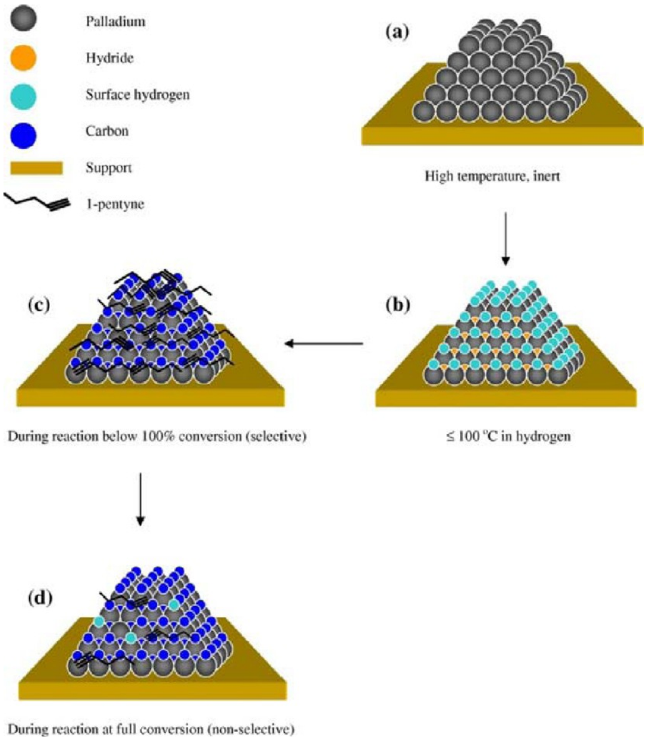

Figure 3. Surface modification with reaction conditions: (a) bare palladium nanoparticles, (b) formation of surface hydrogen and hydride under hydrogen, (c) formation of palladium carbide-like phase during the selective hydrogenation, and (d) carbide during non-selective hydrogenation. Reprinted from 47 with permission from Elsevier.

kept in mind that these systems are composed of supported metal nanoparticles and that the former can also have an influence on the C-laydown deposition phenomenon.

2.1.2. Active Phase Modification. The yield of the olefinic hydrogenation product is known to increase significantly with the incorporation of additives in the reaction mixture (*reaction modifiers*) or in the catalyst formulation (*catalyst modifiers*). Within the former grouping, reaction modifiers for liquid phase alkyne reactions are typically N or S containing compounds which are added to the reaction medium.[49,51,53,113,114] In gas phase reactions, the addition of CO as a reaction modifier has been extensively used.[32,43] The latter grouping represents the foreign compounds present in the catalyst formulation, which might be remnants of the catalyst preparation (such as stabilizing polymers and/or surfactants) or, for example, a second metal.

A typical example of catalyst modification can be found in Lindlar's (5% w/w Pd/$CaCO_3$ modified by lead acetate and quinoline) catalyst,[115] which since its first appearance in 1952, has been regarded as the reference catalyst in alkyne hydrogenations. A recent publication unravels through DFT calculations how each modification acts to prevent the unwanted side reactions in this system.[97] The addition of Pb as a second metal not only limits the predisposition of Pd to form hydride phases, which are known to be too reactive, and thus unselective, but it also hinders alkene adsorption and thus overhydrogenation.[44,47] Finally, quinoline addition was found to improve selectivity through site-separation, impeding the formation of oligomers.

2.1.2.1. Catalyst Modifiers. The incorporation of stabilizing agents, for example, surfactants, polymers, and dendrimers[107−109,116] (see Table 2) during the preparation process is required for the stabilization of the inherently thermodynamically and kinetically unstable solutions of nanoparticles subsequently used for catalysis. Moreover, shape control implies the use of molecular capping agents which selectively adsorb to one specific crystal plane, thus favoring the addition of metal on the weakly bonded facet and directing the growth of the nanoparticle.[109] Despite the extensive cleaning procedures applied to the obtained nanoparticles, it is common to find traces of the stabilizing and capping agents which modify the true catalytic behavior of the metal.

The presence of PVP as stabilizer for Pd,[16,51] Pt,[55] and Rh[85] has been associated with improved selectivity toward the target alkene because of the electronic modifications of Pd induced by N-containing species. This is in good agreement with results obtained over catalysts permanently modified with bipyridine-based ligands,[49] phenanthroline-based ligands,[56] and copolymers.[69]

Surfactant stabilizing agents[58,64,117] have also been used in alkyne hydrogenations where catalytic performance has been correlated with the charge and the alkyl chain length.[58] Equivalent activity was obtained with CTAB and AOT, in the selective hydrogenation of MBY[64] while lower rates were reported for PVP (relative to AOT)[101] and ascribed to the stronger interaction of the latter with the metal surface. This is consistent with the increased activity (but lower selectivity) in acetylene hydrogenation following PVP removal from supported Pd nanocubes.[16]

Ionic liquids have been recently used as stabilizing media for Pd nanoparticles in the hydrogenation of acetylene,[15] tolane,[60] 1-chloro-4-pentyne,[60] and 3-hexyne[60] with good results. In the case of acetylene hydrogenation, a remarkable selectivity improvement was obtained, avoiding the formation of oligomerization products.[15]

2.1.2.2. Reaction Modifiers. The incorporation of additives to the reaction medium as reaction modifiers has a major drawback compared to catalyst modifiers requiring costly separation and disposal operations. Nitrogen bases, for example quinoline[63,74,114] and pyridine,[67] and sulfur compounds[62,96] are commonly employed.

Nitrogen bases are often included, such as in the case of Lindlar's catalyst. The effect mechanism of the nitrogen organic bases is still far from being resolved but the consensus that emerges from the literature suggests the following:

- A "ligand" effect: a nucleophilic modifier increases the electron density of the palladium surface through electron donation from the coordinating ligand that leads to a change in the alkyne/alkene relative strength of adsorption.[113]
- Poisoning (site blocking) effect: the least selective sites are blocked by irreversibly adsorbed additive molecules.[49]

Tschan et al.[96] studied the effect of different sulfur-based modifiers on the selectivity and activity of amorphous $Pd_{81}Si_{19}$ catalyst in the hydrogenation of 3,7,11,15-tetramethyl-1-hexadecyn-3-ol and concluded enhanced isophytol selectivity with modifiers containing a higher number of heteroatoms.

2.1.2.3. Addition of a Second Metal. Bimetallic nanoparticles have long been recognized for their promoting effect in alkyne hydrogenations where the incorporation of Ag,[13,24,25] Au,[118] Cu,[13] and Ga[24,25] in Pd catalysts served to limit the degree of oligomerization in the hydrogenation of acetylene.

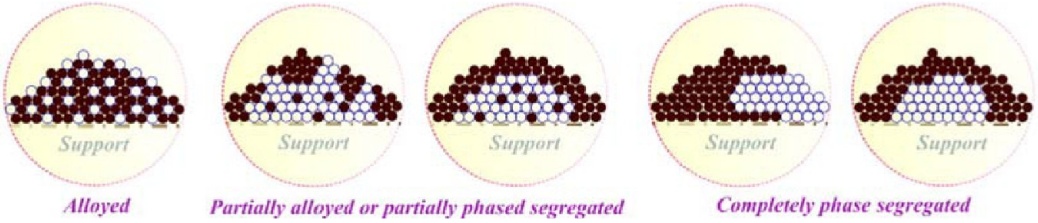

Figure 4. Different possible configurations for bimetallic nanoparticles. Reprinted with permission from ref 119. Copyright (2010) American Chemical Society.

Indeed, the addition of a second metal can be regarded as another form of catalyst permanent modification where different phases can be formed, for example alloy, phase segregation (see Figure 4), depending on several factors such as preparation technique, nature of the two metals and/or the type of support.[119] This could account for the fact that Pd−Ag and Pd−Cu response in the hydrogenation of acetylene was different depending on whether they had been prepared by surface redox or impregnation methods. Furhermore, modification of Pd with Ge, Sb, Sn, or Pb and subsequent treatment at 573 K did not exert any observable effect. If on the other hand, the bimetallic catalysts were treated at 773 K, selectivity decreased for Pb > Sn > Sc modification.[42]

In addition to Pd-containing bimetallic combinations, catalysts based on Cu−Fe,[17,33] Cu−Al,[17,33] Ni−Al,[31] and Ni−Cu[36,43] have also been proved efficient for selective alkyne hydrogenation (see Tables 1 and 2). In fact, DFT calculations found Ni−Zn a viable and substantially less expensive alternative to the classic Pd−Ag system.[23]

A bimetallic active phase can also arise when metallic nanoparticles are deposited on reducible supports. For example, Pd on ZnO has been shown to form an intermetallic PdZn phase even at low temperatures,[46] although the mechanism and the exact morphology of this phase is still not completely understood. PdZn alloy was found to increase selectivity toward the alkene both in liquid[62,63,67] and in gas phase.[46] This effect will be discussed in more depth in the following section.

2.2. Role of the Support: Meso/Microlevel. The effect that supports have on the catalytic performance of the active phase belongs to the meso-level of catalyst design, since the intimate interaction that can arise between them is analogous to that between the active phase and the catalyst modifiers. However, because of its macroscopic nature, the choice of the support also steps into the micro scale length of catalyst design. Indeed, some of its microlevel properties can influence the observed behavior of the catalyst.

The main role of a carrier in supported metal-based catalysts is to anchor the metal nanoparticles to the support to obtain high dispersion, that is, enhanced specific metal surface area and avoid sintering. The key characteristics of a support, critical for catalyst performance can be divided in bulk and surface, chemical (composition and surface chemistry), structural (surface area/porosity, particle size and shape), and mechanical (stability under reaction conditions) properties. Catalytic performance in hydrogen mediated reactions, in general, and the selective alkyne semihydrogenation, in particular, can be controlled by contributions due to the particle size, shape, and electronic properties of the metal phase, as it has been already established in the previous section. These features, in turn, can be affected by interactions with the support. In addition, the nature and strength of the interactions with the support can induce increased metal particle stabilization and avoid undesirable effects such as metal leaching.

2.2.1. Support Effects on Catalysis. 2.2.1.1. Oxides. Oxides are among the most commonly employed carriers for catalytic applications. Frequently used oxide support materials include Al_2O_3, TiO_2, CeO_2, Fe_xO_y, ZrO_2, ZnO (see Tables 1 and 2), all characterized by high decomposition and melting temperatures. The chemical and structural properties of these materials, for example, acid−base and/or redox properties, crystallographic phase, can control the catalytic performance in alkyne hydrogenation via metal−support interactions. A distinct catalytic selectivity (to propene) response and catalyst deactivation has been reported by Lopez-Sanchez and Lennon[30] for the hydrogenation of propyne over Au/Fe_2O_3 and Au/TiO_2. The modified catalytic performance over both systems is ascribed to differences in metal−support interactions where aging and pretreatment conditions play a critical role. Kennedy et al.[28] investigated the hydrogenation of propyne and associated the formation of propene to a hydrocarbonaceous overlayer formed during the early reaction stages. They suggested that distinct metal−support interactions for Al_2O_3 vs SiO_2 supported Pd and Pt impact on the maintenance of this carbonaceous film which in turn impact on the catalytic performance. The structural properties of the support in terms of texture, pore size, and allotropic crystal phase can also impact on the diffusion and adsorption mode of the reactant(s) modifying the catalytic performance. Marín-Astorga et al.[120] studying the hydrogenation of phenyl alkyl acetylenics over a series of siliceous-based (amorphous SiO_2 and mesoporous and silylated MCM-41) supported Pd catalysts ascribed variations in catalytic performance to limitations in terms of access of the reactant molecule to the channels where the highest rate was obtained for Pd/MCM-41 with narrow *meso*-porosity. Using a similar rationale, Alvez-Manoli et al.[57] suggested mesoporosity and differences in textural properties responsible for the increased activity and selectivity over SBA-15, with one-dimensional hexagonal structure, relative to MCM-48 silica and MSU-γ alumina in the hydrogenation of 3-hexyne over a series of Pd-based catalysts. The literature that addresses support effects in terms of crystal phase in alkyne hydrogenation is limited, but Komhom et al.[121] investigated the hydrogenation of acetylene over Pd/Al_2O_3 and showed improved activity and selectivity response over mixed transition- (36%) and α-Al_2O_3 (64%) phases. The presence of transition-phase resulted in a concomitant increase in Brunauer−Emmett−Teller (BET) surface area and Pd dispersion while the α-phase was deemed responsible for the high ethylene selectivity. Differences in the acid/base character of the support can impact on the electronic properties of the supported metal particles. This is illustrated in Figure 5 where the palladium binding energies indicate a gradual decrease in the binding energy with increasing support alkalinity and can be

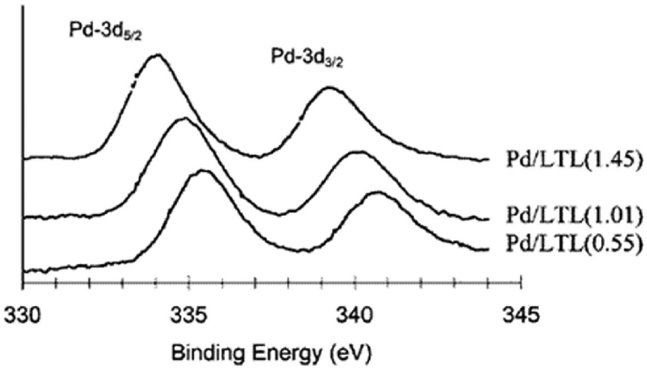

Figure 5. Binding energy of Pd $3d_{5/2}$ and $3d_{3/2}$ for Pd on supports with different acid−base properties. Reprinted from ref 122 with permission from Elsevier.

interpreted as a lowering of the ionization potential of the Pd valence orbitals with increasing alkalinity of the support. Indeed, basic supports enhance the electron density of the metal phase giving rise to $M^{\delta-}$ particles via support→metal electron transfer[123] which in turn results in higher H coverage and metal-H bond strength. It follows that acid carriers can promote the formation of $M^{\delta+}$ particles as a result of metal→support electron transfer whereas the formation of both ($M^{\delta+}$ and $M^{\delta-}$) species is possible in carriers with both basic and acid sites, for example, Al_2O_3.[124] Moreover, the electronic state of the active metal particles can influence the adsorption/activation of polyfunctional organic compounds. Wherli et al.[29] studying the hydrogenation of propyne over Cu-based catalysts prepared by incipient wetness impregnation and/or ion exchange, found a dependence on catalyst deactivation with support acidity. In this respect, because polymerization is acid catalyzed, neutral or basic catalysts reduce catalyst fouling (ZrO_2 > α-Al_2O_3 > γ-Al_2O_3 > SiO_2−Al_2O_3 > SiO_2 > MgO). This was also consistent with the lower deactivation for catalysts with higher dispersion, that is, decrease in the amount of neighboring active sites for the interaction between adsorbed intermediates and propyne resulting in polymerization. The redox characteristics of the oxide support plays also a critical role where partial reduction of carrier can result in (i) partial or total blockage of the active site via migration of suboxide species on top of the metal particles (see Figure 6) and/or (ii) the genesis of new bimetallic phase(s) with modified electronic and geometric properties affecting catalytic performance in the hydrogenation of alkynes. The partial reduction of iron oxide for Au/Fe_xO_y resulted in a decreased selectivity to the target alkene for hydrogen treatment at T > 573 K ascribed to the concomitant partial Fe_3O_4→Fe^0 reduction and formation of Au−Fe ensembles.[9] In the selective hydrogenation of pentyne over Pd/ZnO and Pd/SiO_2 Tew et al.[46] have shown an improved catalytic performance over the former ascribed to the PdZn alloy formation (on the basis of HRXRD, XANES, and EXAFS analyses). The increased selectivity to the alkene product is ascribed to the electronic properties of the alloy which are similar to those of Cu while the lower activity is attributed to a combined surface dilution and particle sintering. In addition to this, other factors such as the presence of impurities have been proved to impact on catalytic performance. In the hydrogenation of propyne over a series of oxide supported Pd catalysts, Jackson and Casey[27] reported 100% selectivity to propene and the following decreasing activity sequence Pd/ZrO_2 > Pd/SiO_2 > Pd/Al_2O_3 where the lower activity recorded over the former was ascribed to the presence of residual chlorine on the surface.

2.2.1.2. Carbonaceous. The carbonaceous material that can be deposited on a catalytic surface is normally amorphous, however, carbon can exist in many different forms such as structured carbon nanofibers and nanospheres, porous, or diamond (see Figure 7). Activated carbon is commonly used as carbon-based material because of the combined high specific surface area (SSA; > 600 m^2 g^{-1}), adsorption capacity, and cost effectiveness.[127] Graphite is the most stable phase in bulk form under ambient conditions.[128] It is characterized by a crystal structure based on layers where carbon atoms are arranged in hexagonal packing with low SSA.[128] The distinct structural properties of these carbon materials can have an effect in the hydrogenation of alkynes, and we have demonstrated[14] for a series of carbon supported Pd catalysts an increase in activity in the acetylene hydrogenation ascribed to enhance metal−support interactions in the more graphitized support. Whereas the limited porosity, that is, low SSA, has restricted the use of graphite for catalytic applications,[129] the significant micropore content of activated carbon can result in physical transport limitations. In this case, the diffusion of the reactant within the microporous structure is slow, thus controlling the overall transformation rate and often affecting the target product selectivity. Graphitic nanofibers represent a group of structured carbon materials with unique catalytic properties. They exhibit a high length relative to width (aspect) ratio characterized by

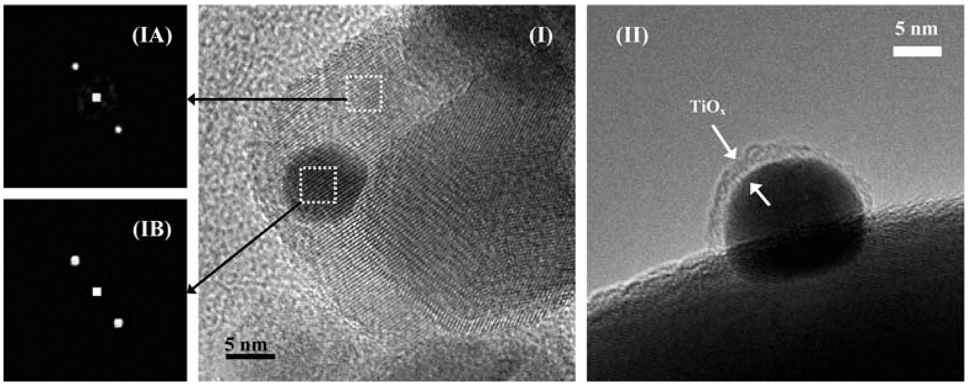

Figure 6. High-resolution TEM images of (I and II) Au/TiO2 with diffractrogam patterns (IA and IB) for the selected (dashed) areas. Note: Arrows in image (II) indicate TiOx layer covering an isolated Au particle. Reprinted from ref 125 with permission from Elsevier.

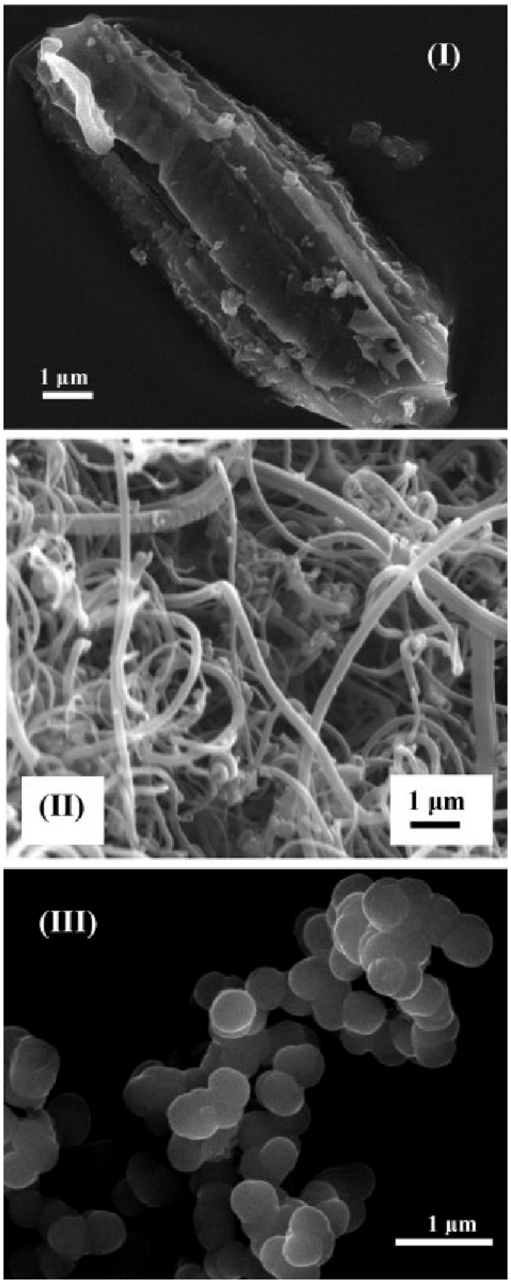

Figure 7. SEM Image of (I) amorphous activated carbon, and structured carbon(II) nanofibers and (III) nanospheres. Reprinted from ref 126 with permission from Elsevier.

arranged layers of graphene, large SSA (10−200 m^2 g^{-1}) and preponderance of edges in the basal and lattice regions that provide enhanced metal−support interactions.[130]

Group VIII noble metals are known to be effective C≡C hydrogenation catalysts (see Tables 1 and 2). However, the chemical inertness of carbon, that is, low surface reactivity, is the main drawback in terms of metal deposition.[128] The surface chemistry and adsorption properties of carbon can be modified by the incorporation of functionalities. The treatment with oxidizing agents in gas (e.g., ozone or carbon dioxide) or liquid (e.g., HNO_3, HCl, H_2O_2) phase is a common *pre*-treatment used to modify the carbon surface chemistry by introducing oxygen-containing groups.[131] This can have a direct effect on the ultimate metal−support interaction(s) where lower activity in the hydrogenation of acetylene over Pd/C for smaller particles (<3 nm) has been reported elsewhere.[14] In the same line, Ryndin et al.[18] studying the hydrogenation of acetylene and vinylacetylene over Pd/C demonstrated a similar activity trend in both reactions and equivalent to that over oxide supported catalysts. The catalytic performance was consistent with an increase in activity over larger Pd particles (>3 nm) with similar electronic properties close to those of bulk (on the basis of XPS). The presence of surface oxygen groups can also influence catalytic performance by modification of the mode/strength of reactant adsorption. Avoidance of undesired hydrogenolysis and isomerization reactions was reported by Musolino and co-workers[70] in the hydrogenation of 2-butyne-1,4-diol for Pd supported on carbon and ascribed to the acid modification process, that is, reduction in the number of impurities and increase in surface oxygen groups. In the hydrogenation of 2-hexyne, Klasovsky et al.[53] associated the lack of activity over some of the carbon supported Pd catalysts under investigation to the presence of impurities, for example, transition metals, ash content, and/or surface acidity, in the carbon raw material.

2.2.1.3. Others. In the search of alternative catalytic systems for alkyne hydrogenation, promising results have been obtained with bulk materials such as nitrides[132] and *non*-noble metal based hydrotalcites (HT).[17,31−33,43] Indeed, in a series of publications, Pérez-Ramirez et al.[17,31−33,43] have shown the catalytic potential of HT-based catalysts for partial *semi*-hydrogenation of unsaturated hydrocarbons, that is, mono-alkynes and dienes. In the selective hydrogenation of propyne, they reported an improved catalytic performance over Ni-[31] and Cu−Al[33] HT relative to the equivalent Al_2O_3 and/or SiO_2 supported (Ni and Cu) catalysts where *pre*-treatment conditions, in terms of calcination/reduction, and metal dispersion play a critical role with increased activity over the most dispersed systems. The formation of C-containing species during the early reaction stages[31] or induced by CO addition[17] favors selectivity to the target alkene although coke formation results in severe catalyst deactivation.[31] Using the same model molecule, they achieved 100% selectivity at increased conversion over ternary Cu−Ni−Fe and proposed that Cu was the hydrogenation metal while Ni increased hydrogen content and Fe acted as structural promoter. Because catalytic performance in C≡C hydrogenation over supported metal systems can be governed by contributions due to the nature of the support, alternative carriers have been proposed. Duca et al.[20] employed pumice with surface alkali metal ions, that increased the electronic density of the metal particles, as a support for Pd. They achieved a compromise between activity/selectivity and stability, comparable to standard oxide supported catalysts, in the treatment of typical industrial acetylene plus alkene mixture feedstocks. Similar catalytic results were obtained for different Pd size, space velocities, and H_2/C_2H_2 ratios where a reaction mechanism was proposed consistent with the existence of two types of surface sites. More recently, Liu et al.[133] have proposed the use of a polymeric support material for Pd on the bases of high surface area, transparency in IR, and preferred condensation of reactants and reaction products where the reaction occurs in a liquid-like phase. They studied the hydrogenation of phenylacetylene by in situ FTIR spectroscopy and observed similar reaction rates over repeated catalytic runs achieving close to 100% alkene selectivity when hydrogen is not in large excess.

2.2.2. Structured Supports. Support effects have classically been studied on powdered catalysts[123] with associated disadvantages in the macro-scaled level during the incorporation in chemical reactors. Conventionally, the choice of the reactor for a given catalytic process revolved around the best catalyst formulation identified for the specific application. This approach is undergoing a shift toward a more efficient parallel process development in which both the macro and microlevels of catalyst design are taken into consideration simultaneously, and where the catalyst is sometimes adapted to the requirements of the reactor.[134] As a result, much effort is at present devoted to the development of structured catalysts that allow the design and operation of more efficient and intrinsically safer reactors. Structured and/or arranged catalysts, for example, monoliths, foams, fibers, corrugated plates, or membranes (Figure 8) bring some advantages as compared to the typical stirred tank and packed bed reactors in both continuous and batch reactors.[2] Indeed, a more efficient multiphase contact is ensured thus allowing operating in kinetic regime at the highest possible reaction rate, resulting in process intensification.

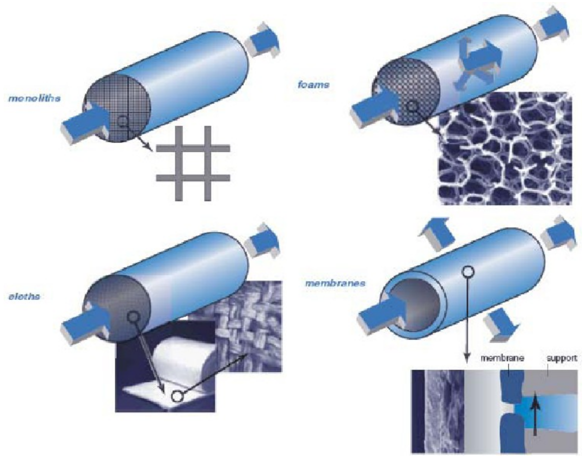

Figure 8. Different types of macrostructured catalysts (monoliths, foams, cloths, and membranes). Adapted with permission from ref 91. Copyright 2003 Springer.

2.3. Process Intensification: Milli/Macro-Level. When going a step further in the RCD approach, the macroscopic level is reached, in which catalyst and reactor must be designed *in unison*. At this point, and to intensify the catalytic process, the most efficient macrostructured catalytic material must be coupled with optimal reactor design and operating conditions.[2,135,136] Industrial catalytic hydrogenations are commonly performed either in fixed-bed reactors or in suspension reactors, such as fluidized beds and mechanical stirred tank reactors,[136,137] as it can be appreciated in Tables 1 and 2. However, these systems present several drawbacks. In the former, the random distribution of the catalyst particles leads to high pressure drop, inhomogeneous flow patterns, broad residence time distributions, and thermal instabilities which results in high energy consumption, thus diminishing the overall process performance.[2,135,136] Moreover, mass transfer limitations are a typical issue in these systems.

Nowadays, industrial requirements are continuously shifting toward continuous operation, where heat management inside the reactor is a decisive issue, especially for highly exothermic reactions such as hydrogenation reactions. Nonetheless, selectivity must also be kept in mind when designing the catalyst/reactor pair. Reactions operated in batch reactors, where appropriate heat management is possible, suffer from catalyst abrasion and limitations in terms of catalyst separation and selectivity loss due to backmixing.[2,136] The proposed solutions involve a process intensification approach, aiming at developing compact, safe, energy-efficient, and environment-friendly processes.[138] Innovative reactor designs include macro and microstructured supports and reactors as well as microreactors, where the main challenge resides in the immobilization of the catalytically active phase.

2.3.1. Macrostructured Catalysts. *Monoliths* are ceramic or metallic structures that contain a multitude of horizontal narrow channels in a single block. They can be produced by either extrusion of the support or adherence of the support/catalyst system onto the monolithic structure.[135] Monolithic reactors are characterized by low pressure drop, no catalyst attrition, reasonable costs, and easy scale-up.[135] The possibility of establishing a well-defined flow regime (Taylor or slug flow) inside the channels for co-current gas–liquid flow provides several advantages, that is, limited degree of back mixing, mass transfer improved by the internal circulation in the liquid phase, and low power consumption.[137] As a result of the poor radial heat transfer, monoliths are often operated as loop reactors with external heat exchangers or as single pass columns with interstage cooling, which diminishes backmixing and, in turn, increases selectivity.[139] Nijhuis et al.[72] investigated the selective liquid-phase hydrogenation of 3-methyl-1-pentyn-3-ol using Pd on a silica monolithic body. They suggested a rational design of a monolithic reactor with narrower channels and predicted it to yield an activity of roughly a 40% of the highest activities obtained with slurry catalysts. Bakker et al.[75] used high-porosity monoliths coated with silica and showed that higher activity and selectivity can be obtained compared to monoliths with impermeable wall in the case of internal diffusion limitations. In both cases, the experiments were carried out in a monolithic stirrer reactor, which can be seen as an attractive alternative to conventional stirred tank slurry reactors.

Fibrous catalysts consist of an active phase immobilized on metal (or coated-metal), glass, or activated carbon fibers. This type of catalytic material is flexible, versatile, easy to handle, and possesses excellent mass transfer performance with low pressure drops. As a result, they can be easily integrated in various shape multifunctional reactors.[140] Our group investigated the potential of sintered metal fibers (SMFs) with high porosity, good redistribution properties, good mechanical strength, and high thermal conductivity, in a series of C$\equiv$C to C$=$C hydrogenations. A structured Pd/ZnO/SMF catalyst was tested in the selective liquid-phase hydrogenation of 2-methyl-3-butyn-2-ol[62,63] where increased activity (by 1 order of magnitude) was attained relative to commercial powder Lindlar's catalyst.[63] This structured catalyst was subsequently integrated in a novel reactor concept based on a bubble column staged by structured catalytic layers with integrated cross-flow microheat-exchangers. Because the combined possibility of high catalyst loading, efficient evacuation of heat, and continuous plug flow operation, the specific productivity of the process could be improved by 2 orders of magnitude compared to conventional multiphase reactors typically used for this reaction.[68]

A less common type of macrostructured catalyst is based on a *foam* material with interconnecting pores that allows lower pressure drop and increased thermal conductivity (metal or SiC foams) than packed-bed reactors.[136] Nonetheless, this technology is still at the research stage where the associated high cost and low surface area are clear drawbacks. Na-Chiangmai et al.[82]

investigated the catalytic properties of an ultralarge pore mesocellular foam silica in the liquid-phase selective hydrogenation of phenylacetylene.

As an alternative to the above-mentioned technologies, *catalytic membranes* allow a distributed addition of reactants or removal of products[91] although the lifetime and regeneration capability still needs further investigation. Lange et al.[54] tested catalytically active microporous thin film membranes for the selective hydrogenation of 2-hexyne where significantly higher selectivity was obtained compared to conventional batch catalysts as a result of the suppression of the contact between the highly reactive intermediate and hydrogen.

2.3.2. Process Intensification Through the Use of Microreactors. Microreactors are miniaturized open-flow reactors with channel dimensions in the submillimeter range offering the possibility of integrating several modules/plates to perform various unit operations, for example, mixing, reaction, heat exchange, and separation, in a single process.[138] Moreover, while conventional contactors have several problems for fast and highly exothermic hydrogenation reactions, microreactors are suitable since mass and heat transfer processes can be accelerated by more than 1 order of magnitude.[136] For gas-phase reactions, randomly micro/milli-packed beds are often used for catalyst optimization and kinetic measurements; however, they suffer from high pressure drop associated with the small particles.[40,43] The most common type is the catalytic wall microreactor.[136] Capillary microreactors wall-coated with mesoporous titania thin films containing embedded nanoparticles were tested in the liquid-phase hydrogenation of 2-methyl-3-butyne-2-ol[67] where higher selectivity at increased conversion and increased stability was obtained compared to batch operation. De Loos et al.[73] tested a microreactor coated with layers of carbon nanofibers in the liquid-phase hydrogenation of 3-methyl-1-pentyn-3-ol and demonstrated that the catalytic layers do not affect the flow regime type. They successfully increased activity by 4 times relative to an unsupported flat plate catalyst.

3. INTEGRATED MULTI-LEVEL APPROACH IN CATALYTIC ALKYNE HYDROGENATIONS: 2-METHYL-3-BUTYN-2-OL AS A CASE STUDY

In the previous sections, we have reviewed separately the state of the art in the different levels involved in process design, from the active site to the reactor. This has been the general trend where RCD has been performed on a single scale length with very limited examples in the literature where an *integrated* approach for RCD was employed. In this sense, it is worth noting the work of Centi and Perathoner[91] who established the grounds for this approach in 2003.

In this section, we illustrate the benefits of this approach by presenting the results in the industrially relevant selective hydrogenation of MBY over Pd-based catalysts over multiple levels in an integrated manner as a case study.

The catalyst's properties have been tuned-on-demand by first identifying the active sites responsible for the catalytic performance, that is, nanolevel design.[61] To do so, well-defined PVP-stabilized Pd nanoparticles with different shapes and sizes were synthesized and tested. Two types of active sites were identified: plane atoms (σ_1) and edge atoms (σ_2), see Figure 2. The results suggested that MBY adsorbs on all types of surface atoms, but its reactivity depends on the coordination number of the active site. The kinetic modeling was performed using a two-site Langmuir–Hinshelwood mechanism with one single set of kinetic and adsorption constants specific to the reaction path or adsorption equilibrium of a compound on a given active site. Good correlation between experimental and predicted (from modeling) results was obtained which, in turn, allowed identifying the optimum Pd active phase in terms of size and shape.

When taking a step further in the rational design of catalysts, one stumbles upon the *meso-level* design of catalysts, in which the interaction between the active phase and the compounds with which it is in intimate contact is investigated. A similar model based on two type of active sites was applied to AOT-stabilized Pd nanocrystals to elucidate the effect of the stabilizing agents surrounding the active phase.[101] For a series of Pd nanocrystals with different morphology we found that nanoparticles with the same shape and size are an order of magnitude more active than those stabilized by PVP. This was tentatively linked to the stronger interaction of PVP with Pd surface atoms as compared to AOT. Furthermore, the selectivity toward the alkene was also modified by the nature of the stabilizer.

During the long process of catalyst development the identification of a catalytically active phase is the first but not the last step. To step into the micro/milli-level catalyst design we deposited the *pre*-optimized active phase on micro-structured materials with tuned surface properties, morphology, and micro/meso-porosity. Three-dimensional sintered metal fibers (SMF) were chosen as a structured support for the deposition of the active Pd nanoparticles (synthesized ex-situ). The SMF was coated with a thin ZnO layer which gave rise to the active/selective catalytic phase of Pd/PdZn/ZnO through metal–support interactions. The catalyst exhibited 1 order of magnitude higher activity, relative to the commercial Lindlar catalyst, proving a yield >95% to the target olefin product.[62,63]

The milli/macro-level catalyst design is closely linked to the reactor development and refers to the macrostructured material conjugated with the development of a complex system aiming at process intensification via improved multiphase contact and heat transfer management. A novel reactor based on a bubble column staged (SBCR) with structured catalytic layers of Pd/ZnO/SMF with integrated cross-flow microheat-exchangers (HEX) was designed and tested in the continuous three-phase hydrogenation of MBY.[68] The reactor (Figure 9) demonstrated high specific productivity under isothermal conditions. The attained specific reactor performance was found to be several orders of magnitude above the values reported for conventional multiphase reactors.

4. SUMMARY AND OUTLOOK

In this review, we show how conventional process design of selective alkyne hydrogenations has been hitherto focused on optimizing the catalyst formulation, leaving the issue of reactor design to be considered in a subsequent step. A more *rational* approach, however, would address the various scale lengths and levels of complexity simultaneously, starting from a molecular/nanoscale involving the active phase optimization up-to a macro-scaled design of the catalytic reactor conjugated with the optimization of operation conditions.

To optimize the catalyst at a nano level, the nature of active sites required for a given reaction must be identified and characterized. This can be achieved under real operational conditions by controlling metal nanoparticle size and shape through colloidal techniques, which provide a simple means of producing nanoparticles on demand. The opportunities seem

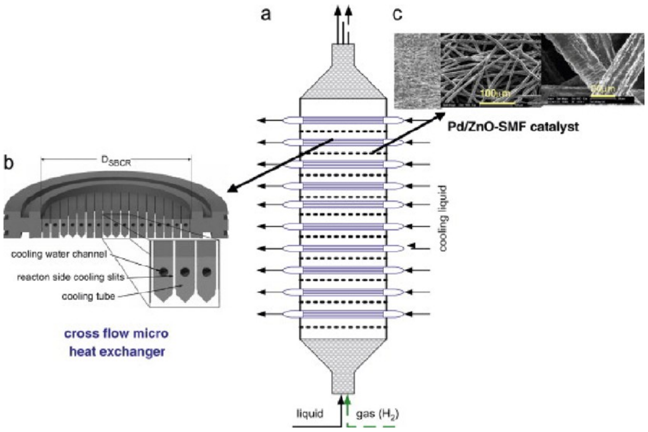

Figure 9. Setup for the continuous hydrogenation of MBY. (a) Staged bubble column reactor (SBCR) with integrated catalyst layers and microheat-exchangers (HEX), (b) transverse plane through the heat-exchanger element, and (c) Pd/ZnO/SMF catalyst. Reprinted from ref 68 with permission from Elsevier.

countless given the large pool of organic stabilizers available to produce metal nanoparticles capable of bridging the material gap between single crystals and industrial catalysts.

The control of the active phase interaction with a support is essential in the catalyst "architecture". The choice of a suitable support can be considered as meso-milli scaled catalyst design taking into consideration the possible chemical interactions with the active phase. However, support development is currently also stepping into a macro-scaled catalyst design since joint catalyst-reactor development is now in vogue. In this sense, new trends point toward functionalized structured supports which are easily included in new and innovating reactor configurations.

Green and safe processes have been a perennial objective in the chemical industry. Research efforts in this direction include process intensification which often implies a switch from batch to continuous operation. This paradigm shift raises new challenges, that is, heat management in the reactor, which have been tackled with the development of creative reactor/catalyst configurations such as loop reactors, staged bubble column reactors, and microreactors.

This review concludes with a case study of alkyne hydrogenation process development performed in our group where we show the importance of addressing all the scale lengths simultaneously as opposed to the classical step-by-step approach.

Although much work has been conducted in triple bond hydrogenations, the forever evolving pace of the field of catalyst design is opening new and exciting ways toward catalyst customization for safer processes.

■ AUTHOR INFORMATION

Corresponding Author

*E-mail: lioubov.kiwi-minsker@epfl.ch. Phone: +41 21 693 3182. Fax: +41 21 693 3667.

Notes

The authors declare no competing financial interest.

■ REFERENCES

(1) Jiménez-González, C.; Poechlauer, P.; Broxterman, Q. B.; Yang, B.-S.; Ende, D. A.; Baird, J.; Bertsch, C.; Hannah, R. E.; Dell'Orco, P.; Noorman, H.; Yee, S.; Reintjens, R.; Wells, A.; Massonneau, V.; Manley, J. *Org. Process Res. Dev.* **2011**, *15*, 900.

(2) Kiwi-Minsker, L.; Crespo-Quesada, M. *Chimia* **2011**, *65*, 699.

(3) Ozkan, U. S. *Design of heterogeneous catalysts*; Wiley-VCH: Weinheim, Germany, 2009.

(4) Chen, B.; Dingerdissen, U.; Krauter, J. G. E.; Rotgerink, H. G. J. L.; Möbus, K.; Ostgard, D. J.; Panster, P.; Riermeier, T. H.; Seebald, S.; Tacke, T.; Trauthwein, H. *Appl. Catal., A* **2005**, *280*, 17.

(5) Ulan, J. G.; Kuo, E.; Maier, W. F.; Rai, R. S.; Thomas, G. *J. Org. Chem.* **1987**, *52*, 3126.

(6) Ghosh, A. K.; Krishnan, K. *Tetrahedron Lett.* **1998**, *39*, 947.

(7) Jung, A.; Jess, A.; Schubert, T.; Schütz, W. *Appl. Catal., A* **2009**, *362*, 95.

(8) Jia, J. F.; Haraki, K.; Kondo, J. N.; Domen, K.; Tamaru, K. *J. Phys. Chem. B* **2000**, *104*, 11153.

(9) Sárkány, A.; Schay, Z.; Frey, K.; Széles, É.; Sajó, I. *Appl. Catal., A* **2010**, *380*, 133.

(10) Azizi, Y.; Petit, C.; Pitchon, V. *J. Catal.* **2008**, *256*, 338.

(11) Choudhary, T. V.; Sivadinarayana, C.; Datye, A. K.; Kumar, D.; Goodman, D. W. *Catal. Lett.* **2003**, *86*, 1.

(12) Zhang, Q. W.; Li, J.; Liu, X.; Zhu, Q. *Appl. Catal., A* **2000**, *197*, 221.

(13) Kim, S. K.; Lee, J. H.; Ahn, I. Y.; Kim, W.-J.; Moon, S. H. *Appl. Catal., A* **2011**, *401*, 12.

(14) Tribolet, P.; Kiwi-Minsker, L. *Catal. Today* **2005**, *105*, 337.

(15) Ruta, M.; Laurenczy, G.; Dyson, P. J.; Kiwi-Minsker, L. *J. Phys. Chem. C* **2008**, *112*, 17814.

(16) Crespo-Quesada, M.; Andanson, J.-M.; Yarulin, A.; Lim, B.; Xia, Y.; Kiwi-Minsker, L. *Langmuir* **2011**, *27*, 7909.

(17) Bridier, B.; Pérez-Ramírez, J. *J. Am. Chem. Soc.* **2010**, *132*, 4321.

(18) Ryndin, Y. A.; Stenin, M. V.; Boronin, A. I.; Bukhtiyarov, V. I.; Zaikovskii, V. I. *Appl. Catal.* **1989**, *54*, 277.

(19) Sárkány, A.; Weiss, A. H.; Guczi, L. *J. Catal.* **1986**, *98*, 550.

(20) Duca, D.; Frusteri, F.; Parmaliana, A.; Deganello, G. *Appl. Catal., A* **1996**, *146*, 269.

(21) Borodziński, A.; Gołębiowski, A. *Langmuir* **1997**, *13*, 883.

(22) Borodziński, A.; Cybulski, A. *Appl. Catal., A* **2000**, *198*, 51.

(23) Studt, F.; Abild-Pedersen, F.; Bligaard, T.; Sørensen, R. Z.; Christensen, C. H.; J. K. Nørskov, J. K. *Science* **2008**, *320*, 1320.

(24) Osswald, J.; Giedigkeit, R.; Jentoft, R. E.; Armbrüster, M.; Girgsdies, F.; Kovnir, K.; Ressler, T.; Grin, Y.; Schlögl, R. *J. Catal.* **2008**, *258*, 210.

(25) Osswald, J.; Kovnir, K.; Armbrüster, M.; Giedigleit, R.; Jentoft, R. E.; Wild, U.; Grin, Y.; Schlögl, R. *J. Catal.* **2008**, *258*, 219.

(26) Nikolaev, S. A.; Permyakov, N. A.; Smirnov, V. V.; Vasil'kov, A. Y.; Lanin, S. N. *Kinet. Catal.* **2010**, *51*, 288.

(27) Jackson, S. D.; Casey, N. J. *J. Chem. Soc., Faraday Trans.* **1995**, *91*, 3269.

(28) Kennedy, D. R.; Webb, G.; Jackson, S. D.; Lennon, D. *Appl. Catal., A* **2004**, *259*, 109.

(29) Wehrli, J. T.; Thomas, D. J.; Wainwright, M. S.; Trimm, D. L.; Cant, N. W. *Appl. Catal.* **1991**, *70*, 253.

(30) López-Sánchez, J. A.; Lennon, D. *Appl. Catal., A* **2005**, *291*, 230.

(31) Abellò, S.; Verboekend, D.; Bridier, B.; Pérez-Ramírez, J. *J. Catal.* **2008**, *259*, 85.

(32) Bridier, B.; Hevia, M. A. G.; López, N.; Pérez-Ramírez, J. *J. Catal.* **2011**, *278*, 167.

(33) Bridier, B.; López, N.; Pérez-Ramírez, J. *J. Catal.* **2010**, *269*, 80.

(34) Wehrli, J. T.; Thomas, D. J.; Wainwright, M. S.; Trimm, D. L.; Cant, N. W. *Appl. Catal.* **1990**, *66*, 199.

(35) Mann, R. S.; Khulbe, K. C. *J. Catal.* **1968**, *10*, 401.

(36) Mann, R. S.; Khulbe, K. C. *Indian J. Technol.* **1973**, *11*, 262.

(37) Maetz, P.; Touroude, R. *Catal. Lett.* **1990**, *4*, 37.

(38) Maetz, P.; Guerrero, G. D.; Touroude, R. *React. Kinet. Catal. Lett.* **1993**, *51*, 293.

(39) Maetz, P.; Touroude, R. *J. Mol. Catal.* **1994**, *91*, 259.

(40) Koeppel, R. A.; Wehrli, J. T.; Wainwright, M. S.; Trimm, D. L.; Cant, N. W. *Appl. Catal., A* **1994**, *120*, 163.

(41) Wehrli, J. T.; Thomas, D. J.; Wainwright, M. S.; Trimm, D. L.; Cant, N. W. *Stud. Surf. Sci. Catal.* **1993**, *75*, 2289.

(42) Aduriz, H. R.; Bodnariuk, P.; Coq, B.; Figueras, F. *J. Catal.* **1991**, *129*, 47.

(43) Bridier, B.; J. Pérez-Ramírez, J. *J. Catal.* **2011**, *284*, 165.

(44) Teschner, D.; Vass, E.; Hävecker, M.; Zafeiratos, S.; Schnörch, P.; Sauer, H.; Knop-Gericke, A.; Schlögl, R.; Chamam, M.; Wootsch, A.; Canning, A. S.; Gamman, J. J.; Jackson, S. D.; McGregor, J.; Gladden, L. F. *J. Catal.* **2006**, *242*, 26.

(45) Teschner, D.; Borsodi, J.; Wootsch, A.; Révay, Z.; Hävecker, M.; Knop-Gericke, A.; Jackson, S. D.; Schlögl, R. *Science* **2008**, *320*, 86.

(46) Tew, M. W.; Emerich, H.; Bokhoven, J. A. v. *J. Phys. Chem. C* **2011**, *115*, 8457.

(47) Tew, M. W.; Janousch, M.; Huthwelker, T.; Bokhoven, J. A. v. *J. Catal.* **2011**, *283*, 45.

(48) Semagina, N.; Renken, A.; Kiwi-Minsker, L. *J. Phys. Chem. C* **2007**, *111*, 13933.

(49) Crespo-Quesada, M.; Dykeman, R. R.; Laurenczy, G.; Dyson, P. J.; Kiwi-Minsker, L. *J. Catal.* **2011**, *279*, 66.

(50) Anderson, J. A.; Mellor, J.; Wells, R. P. K. *J. Catal.* **2009**, *261*, 208.

(51) Evangelisti, C.; Panziera, N.; D'Alessio, A.; Bertinetti, L.; Botavina, M.; Vitulli, G. *J. Catal.* **2010**, *272*, 246.

(52) Mastalir, A.; Rac, B.; Kiraly, Z.; Tasi, G.; Molnar, A. *Catal. Commun.* **2008**, *9*, 762.

(53) Klasovsky, F.; Claus, P.; Wolf, D. *Top. Catal.* **2009**, *52*, 412.

(54) Lange, C.; Storck, S.; Tesche, B.; Maier, W. F. *J. Catal.* **1998**, *175*, 280.

(55) Lange, C.; De Caro, D.; Gamez, A.; Storck, S.; Bradley, J. S.; Maier, W. F. *Langmuir* **1999**, *15*, 5333.

(56) Schmid, G.; Emde, S.; Maihack, V.; MeyerZaika, W.; Peschel, S. *J. Mol. Catal. A: Chem.* **1996**, *107*, 95.

(57) Alvez-Manoli, G.; Pinnavaia, T. J.; Zhang, Z.; Lee, D. K.; Marín-Astorga, K.; Rodriguez, P.; Imbert, F.; Reyes, P.; Marín-Astorga, N. *Appl. Catal., A* **2010**, *387*, 26.

(58) Bonnemann, H.; Brijoux, W.; Siepen, K.; Hormes, J.; Franke, R.; Pollmann, J.; Rothe, J. *Appl. Organomet. Chem.* **1997**, *11*, 783.

(59) Mastalir, A.; Kiraly, Z.; Patzko, A.; Dekany, I.; L'Argentiere, P. *Carbon* **2008**, *46*, 1631.

(60) Venkatesan, R.; Prechtl, M. H. G.; Scholten, J. D.; Pezzi, R. P.; Machado, G.; Dupont, J. *J. Mater. Chem.* **2011**, *21*, 3030.

(61) Crespo-Quesada, M.; Yarulin, A.; Jin, M.; Xia, Y.; Kiwi-Minsker, L. *J. Am. Chem. Soc.* **2011**, *133*, 12787.

(62) Crespo-Quesada, M.; Grasemann, M.; Semagina, N.; Renken, A.; Kiwi-Minsker, L. *Catal. Today* **2009**, *147*, 247.

(63) Semagina, N.; Grasemann, M.; Xanthopoulos, N.; Renken, A.; Kiwi-Minsker, L. *J. Catal.* **2007**, *251*, 213.

(64) Semagina, N.; Kiwi-Minsker, L. *Catal. Lett.* **2009**, *127*, 334.

(65) Semagina, N.; Renken, A.; Laub, D.; Kiwi-Minsker, L. *J. Catal.* **2007**, *246*, 308.

(66) Protasova, L. N.; Rebrov, E. V.; Choy, K. L.; Pung, S. Y.; Engels, V.; Cabaj, M.; Wheatley, A. E. H.; Schouten, J. C. *Catal. Sci. Technol.* **2011**, *1*, 768.

(67) Rebrov, E. V.; Klinger, E. A.; Berenguer-Murcia, A.; Sulman, E. M.; Schouten, J. C. *Org. Process Res. Dev.* **2009**, *13*, 991.

(68) Grasemann, M.; Renken, A.; Kashid, M.; Kiwi-Minsker, L. *Chem. Eng. Sci.* **2010**, *65*, 364.

(69) Semagina, N.; Joannet, E.; Parra, S.; Sulman, E.; Renken, A.; Kiwi-Minsker, L. *Appl. Catal., A* **2005**, *280*, 141.

(70) Musolino, M. G.; Cutrupi, C. M. S.; Donato, A.; Pietropaolo, D.; Pietropaolo, R. *J. Mol. Catal. A: Chem.* **2003**, *195*, 147.

(71) Telkar, M. M.; Rode, C. V.; Chaudhari, R. V.; Joshi, S. S.; Nalawade, A. M. *Appl. Catal., A* **2004**, *273*, 11.

(72) Nijhuis, T. A.; van, K. G.; Moulijn, J. A. *Appl. Catal., A* **2003**, *238*, 259.

(73) de Loos, S. R. A.; van der Schaaf, J.; de Croon, M. H. J. M.; Nijhuis, T. A.; Schouten, J. C. *Chem. Eng. J.* **2012**, *179*, 242.

(74) Spee, M. P. R.; Boersma, J.; Meijer, M. D.; Slagt, M. Q.; van, K. G.; Geus, J. W. *J. Org. Chem.* **2001**, *66*, 1647.

(75) Bakker, J. J. W.; Groendijk, W. J.; de Lathouder, K. M.; Kapteijn, F.; Moulijn, J. A.; Kreutzer, M. T.; Wallin, S. A. *Ind. Eng. Chem. Res.* **2007**, *46*, 8574.

(76) Hori, J.; Murata, K.; Sugai, T.; Shinohara, H.; Noyori, R.; Arai, N.; Kurono, N.; Ohkuma, T. *Adv. Synth. Catal.* **2009**, *351*, 3143.

(77) Mastalir, A.; Kiraly, Z. *J. Catal.* **2003**, *220*, 372.

(78) Mastalir, A.; Kiraly, Z.; Berger, F. *Appl. Catal., A* **2004**, *269*, 161.

(79) Dominguez-Dominguez, S.; Berenguer-Murcia, A.; Linares-Solano, A.; Cazorla-Amoros, D. *J. Catal.* **2008**, *257*, 87.

(80) Dominguez-Dominguez, S.; Berenguer-Murcia, W.; Pradhan, B. K.; Linares-Solano, A.; Cazorla-Amoros, D. *J. Phys. Chem. C* **2008**, *112*, 3827.

(81) Jackson, S. D.; Shaw, L. A. *Appl. Catal., A* **1996**, *134*, 91.

(82) Na-Chiangmai, C.; Tiengchad, N.; Kittisakmontree, P.; Mekasuwandumrong, O.; Powell, J.; Panpranot, J. *Catal. Lett.* **2011**, *141*, 1149.

(83) Starodubtseva, E. V.; Vinogradov, M. G.; Turova, O. V.; Bumagin, N. A.; Rakov, E. G.; Sokolov, V. I. *Catal. Commun.* **2009**, *10*, 1441.

(84) Galvagno, S.; Poltarzewski, Z.; Donato, A.; Neri, G.; Pietropaolo, R. *J. Mol. Catal.* **1986**, *35*, 365.

(85) Pellegatta, J. L.; Blandy, C.; Colliere, V.; Choukroun, R.; Chaudret, B.; Cheng, P.; Philippot, K. *J. Mol. Catal. A: Chem.* **2002**, *178*, 55.

(86) Molnár, A.; Sárkány, A.; Varga, M. *J. Mol. Catal. A: Chem.* **2001**, *173*, 185.

(87) Borodziński, A.; Bond, G. C. *Catal. Rev. - Sci. Eng.* **2007**, *48*, 91.

(88) Borodziński, A.; Bond, G. C. *Catal. Rev. - Sci. Eng.* **2008**, *50*, 379.

(89) López, N.; Vargas-Fuentes, C. *Chem. Commun.* **2012**, *48*, 1379.

(90) Sie, S. T.; Krishna, R. *Rev. Chem. Eng.* **1998**, *14*, 159.

(91) Centi, G.; Perathoner, S. *Cattech* **2003**, *7*, 78.

(92) Bos, A. N. R.; Westerterp, K. R. *Chem. Eng. Process.* **1993**, *32*, 1.

(93) Mei, D.; Sheth, P. A.; Neurock, M.; Smith, C. M. *J. Catal.* **2006**, *242*, 1.

(94) Rajaram, J.; Narula, A. P. S.; Chawla, H. P. S.; Dev, S. *Tetrahedron* **1983**, *39*, 2315.

(95) García-Mota, M.; Bridier, B.; Perez-Ramirez, J.; Lopez, N. *J. Catal.* **2010**, *273*, 92.

(96) Tschan, R.; Schubert, M. M.; Baiker, A.; Bonrath, W.; Rotgerink, L. H. *Catal. Lett.* **2001**, *75*, 31.

(97) García-Mota, M.; Gomez-Diaz, J.; Novell-Leruth, G.; Vargas-Fuentes, C.; Bellarosa, L.; Bridier, B.; Perez-Ramirez, J.; Lopez, N. *Theor. Chem. Acc.* **2011**, *128*, 663.

(98) Burda, C.; Chen, X.; Narayanan, R.; El-Sayed, M. A. *Chem. Rev.* **2005**, *105*, 1025.

(99) Coq, B.; Figueras, F. *J. Mol. Catal. A: Chem.* **2001**, *173*, 117.

(100) Molnár, A.; Sarkany, A.; Varga, M. *J. Mol. Catal. A: Chem.* **2001**, *173*, 185.

(101) Kiwi-Minsker, L.; Crespo-Quesada, M. *Top. Catal.* **2012**, *55*, 486−491.

(102) Bond, G. C. *Chem. Soc. Rev.* **1991**, *20*, 441.

(103) Boitiaux, J. P.; Cosyns, J.; Vasudevan, S. *Appl. Catal.* **1983**, *6*, 41.

(104) Jujjuri, S.; Ding, E.; Shore, S. G.; Keane, M. A. *J. Mol. Catal. A: Chem.* **2007**, *272*, 96.

(105) Ziemecki, S. B.; Michel, J. B.; Jones, G. A. *React. Solids* **1986**, *2*, 187.

(106) Nag, N. K. *J. Phys. Chem. B* **2001**, *105*, 5945.

(107) Jia, C. J.; Schuth, F. *Phys. Chem. Chem. Phys.* **2011**, *13*, 2457.

(108) Semagina, N.; Kiwi-Minsker, L. *Catal. Rev. - Sci. Eng.* **2009**, *51*, 147.

(109) Tao, A. R.; Habas, S.; Yang, P. D. *Small* **2008**, *4*, 310.

(110) Borodziński, A. *Catal. Lett.* **2001**, *71*, 169.

(111) Gracia, L.; Calatayud, M.; Andres, J.; Minot, C.; Salmeron, M. *Phys. Rev. B* **2005**, 71.

(112) Hartog, A. J. D.; Deng, M.; Jongerius, F.; Ponec, V. *J. Mol. Catal.* **1990**, *60*, 99.

(113) Mallat, T.; Baiker, A. *Appl. Catal., A* **2000**, *200*, 3.

(114) Nijhuis, T. A.; van Koten, G.; Kaptejn, F.; Moulijn, J. A. *Catal. Today* **2003**, *79–80*, 315.
(115) Lindlar, H. *Helv. Chim. Acta* **1952**, *35*, 446.
(116) Xia, Y.; Xiong, Y. J.; Lim, B.; Skrabalak, S. E. *Angew. Chem., Int. Ed.* **2009**, *48*, 60.
(117) Brandão, L.; Fritsch, D.; Mendes, A. M.; Madeira, L. M. *Ind. Eng. Chem. Res.* **2007**, *46*, 377.
(118) Choudary, B. M.; Lakshmi, K. M.; Mahender, R. N.; Koteswara, R. K.; Haritha, Y.; Bhaskar, V.; Figueras, F.; Tuel, A. *Appl. Catal., A* **1999**, *181*, 139.
(119) Wanjala, B. N.; Luo, J.; Loukrakpam, R.; Fang, B.; Mott, D.; Njoki, P. N.; Engelhard, M.; Naslund, H. R.; Wu, J. K.; Wang, L.; Malis, O.; Zhong, C.-J. *Chem. Mater.* **2010**, *22*, 4282.
(120) Marin-Astorga, N.; Pecchi, G.; Fierro, J. L. G.; Reyes, P. *Catal. Lett.* **2003**, *91*, 115.
(121) Komhom, S.; Mekasuwandumrong, O.; Praserthdam, P.; Panpranot, J. *Catal. Commun.* **2008**, *10*, 86.
(122) Mojet, B. L.; Miller, J. T.; Ramaker, D. E.; Koningsberger, D. C. *J. Catal.* **1999**, *186*, 373.
(123) Stakheev, A. Y.; Kustov, L. M. *Appl. Catal., A* **1999**, *188*, 3.
(124) Trueba, M.; Trasatti, S. P. *Eur. J. Inorg. Chem.* **2005**, 3393.
(125) Cárdenas-Lizana, F.; de Pedro, Z. M.; Gomez-Quero, S.; Keane, M. A. *J. Mol. Catal. A: Chem.* **2010**, *326*, 48.
(126) Nieto-Márquez, A.; Gil, S.; Romero, A.; Valverde, J. L.; Gomez-Quero, S.; Keane, M. A. *Appl. Catal., A* **2009**, *363*, 188.
(127) Rodriguez-Reinoso, F. *Carbon* **1998**, *36*, 159.
(128) Mantell, C. L. *Carbon and graphite handbook*; Krieger: Huntington, NY, 1979.
(129) Auer, E.; Freund, A.; Pietsch, J.; Tacke, T. *Appl. Catal., A* **1998**, *173*, 259.
(130) de Jong, K. P.; Geus, J. W. *Catal. Rev. - Sci. Eng.* **2000**, *42*, 481.
(131) Moreno-Castilla, C.; Ferro-García, M. A.; Joly, J. P.; Bautista-Toledo, I.; Carrasco-Marín, F.; Rivera-Utrilla, J. *Langmuir* **1995**, *11*, 4386.
(132) Hao, Z.; Wei, Z.; Wang, L.; Li, X.; Li, C.; Min, E.; Xin, Q. *Appl. Catal., A* **2000**, *192*, 81.
(133) Liu, W.; Arean, C. O.; Bordiga, S.; Groppo, E.; Zecchina, A. *ChemCatChem* **2011**, *3*, 222.
(134) Duduković, M. P.; Larachi, F.; Mills, P. L. *Catal. Rev. - Sci. Eng.* **2002**, *44*, 123.
(135) Moulijn, J. A.; Kapteijn, F.; Stankiewicz, A. In *Re-Engineering the Chemical Processing Plant. Process Intensification*; Stankiewicz, A., Moulijn, J. A., Eds.; CRC Press: Boca Raton, FL, 2003.
(136) Renken, A.; Kiwi-Minsker, L. In *Advances in Catalysis*; Academic Press.: New York, 2010; Vol. *53*.
(137) Kreutzer, M. T.; Kapteijn, F.; Moulijn, J. A. *Catal. Today* **2006**, *111*, 111.
(138) Stankiewicz, A. I.; Moulijn, J. A. *Chem. Eng. Prog.* **2000**, *96*, 22.
(139) Winterbottom, J. M.; Marwan, H.; Stitt, E. H.; Natividad, R. *Catal. Today* **2003**, *79*, 391.
(140) Matatov-Meytal, Y.; Sheintuch, M. *Appl. Catal., A* **2002**, *231*, 1.